CIO 320 Project: Heat and Piping Design for Pyrolysis Fluidised Bed

Group 24

Ahmed Ridaa Kader

16077416

Xandro da Silva

15006931

Nyasha Chideme

15022383

Sipho Zulu

15045634

Department of Chemical Engineering

University of Pretoria

South Africa

CIO 320

2020-12-15

CIO 320 Project: Heat and Piping Design for Pyrolysis Fluidised Bed

Abstract

The growing need of energy in the world is the driving force of innovation. The University of Pretoria has developed a Combustion Reduction Integrated Pyrolysis System (CRIPS), which is a dual fluidised bed fast pyrolyser that converts biomass waste to bio-fuels that have many applications in the industry sector. Two projects on the CRIPS process were conducted. The first CRIPS was conducted by Swart (2013), but the project was more concerned with the design, modelling and the construction of a scalable dual fluidised bed system for the pyrolysis of the biomass. Only the energy balance approach using enthalpy as a reference level was used to model the pyrolysis process for the first CRIPS. Swart (2013) did not give attention to the optimisation of the process or the actual design of the fluidised bed. This resulted in CRIPS 1 experiencing severe energy losses and that prevented CRIPS 1 from performing well.

On the other hand, de la Rey (2015) conducted a study on CRIPS 2 and, unlike in CRIPS 1, the main concern was making the whole process efficient. To further improve the CRIPS 2 design, this report looks at designing and optimising a particular heat exchanger in the system in an effort to find a way to recover bio-oil with minimum energy expense.

Since this is an existing system it was decided to change as little as possible where the fluidised bed and associated equipment are concerned. Small scale pilot plants rarely have extravagant budgets and CRIPS 2 is stated to be optimally designed. The heat exchanger used to preheat the air before feeding it into the bed, however, was not optimally designed.

The heat exchanger was designed and optimised to operate at maximum biomass throughput. This report details the design specifications, method and the substantiations for the choices made. The heat exchanger is still to be housed within the reactor shell and the sand is to be loaded from the top, through the center of the heat exchanger. The refractory was cut to allow for a larger heat exchanger and

There is more that can be done to improve the heat exchange and save even more of the energy, however, the existing construction is limiting and the recommendations include options to feed sand differently, construct the heat exchanger outside the reactor and heat up the synthesis gas before it is fed.

Contents

List of Figures

Nomenclature

f	Darcy frictional factor	
$\Delta P'_f$	Pressure difference due to friction	Pa
ΔP_a	Pressure difference due to fluid movers	Pa
ΔP_{CV}	Pressure difference due to control valves	Pa
ΔP_{EL}	Pressure difference between two elevated points	Pa
ΔP_{EP}	Pressure difference between two points	Pa
ΔP_{EQ}	Pressure difference due to loss equipment and flow measuring equipment	Pa
ΔP_f	Pressure difference due to friction of components in pipe sections	Pa
ΔP_{KE}	Pressure difference due to kinetic energy	Pa
ΔP_{STV}	Sub-total varying temperature difference	Pa
ΔT	Temperature difference	K
ϵ	Absolute pipe roughness	mm
μ	Viscosity	$\mathrm{Pa\,s}$
ρ	Density	$\mathrm{kg\,m^{-3}}$
σ	Stefan-Boltzman constant	$\mathrm{W\,m^{-2}\,K^{-4}}$
ε	Emissivity	
A	Area	$\mathrm{m^2}$
A_{in}	Air Feed Rate	$\mathrm{kg\,h^{-1}}$
B_{in}	Biomass Feed Rate	$\mathrm{kg\,h^{-1}}$
c	Sonic velocity	$\mathrm{m\,s^{-1}}$
C_p	Specific heat capacity where pressure is kept constant	$\mathrm{J\,g^{-1}\,K^{-1}}$
C_v	Specific heat capacity where volume is kept constant	$\mathrm{J\,g^{-1}\,K^{-1}}$
D	Diameter	m
g	Gravitational constant	m

h	Convective heat transfer coefficient	$\mathrm{W\,m^{-2}\,K^{-1}}$
k	Specific heat capacity ratio	
k	Thermal conductivity	$\mathrm{W\,m^{-1}\,K^{-1}}$
L	Length	m
M	Molecular weight	$\mathrm{g\,mol^{-1}}$
Ma	Mach number	
P	Pressure	Pa
Q_{cond}	Conduction	W
Q_{conv}	Convection	W
Q_{rad}	Radiation	W
R	Gas constant	$\mathrm{J\,mol^{-1}\,K^{-1}}$
S	Sand Feed Rate	$\mathrm{kg\,h^{-1}}$
S_{HHV}	Higher Heating Value of Syn Gas	$\mathrm{MJ\,kg^{-1}}$
S_{in}	Syn Gas Feed Rate	$\mathrm{kg\,h^{-1}}$
$\mathrm{S}_{recycle}$	Sand Recycle Stream	$\mathrm{kg\,h^{-1}}$
T	Temperature	
T_{∞}	Ambient temperature	K
T_{air}	Inlet Air Temperature	K
T_{Bed}	Pyrolysis Fluidised Bed Temperature	K
T_{c}	Combustion Chamber Temperature	K
t_{min}	Minimium wall thickness	cm
T_{surr}	Surrounding temperature	K
T_{syn}	Inlet Syn Gas Temperature	K
T_{s}	Surface temperature	K
u	Linear velocity	$\mathrm{m\,s^{-1}}$
W	Mass flow rate	$\mathrm{kg\,s^{-1}}$
z	Compressibilty factor	

1 Introduction

1.1 Background

Fossil fuels have been powering the world for many years. They originate from dead plants and animals that walked this planet million years ago and got buried deep underneath the earth surface where they got converted into combustible material under high pressure and temperature conditions. Currently, human beings are too dependent on fossil fuels using them to heat homes, run cars, power offices, industry and manufacturing sectors. The demand for energy is growing exponentially, but fossil fuels do not replenish fast enough to meet the energy demands.

Scientists and engineers are looking for alternatives for fossil fuels to help ease the energy demands especially in the industry and the manufacturing sectors. According to de la Rey (2015, p. 1), the use of biomass, specifically wood, is a promising replacement. Pyrolysis, which is defined as the thermal decomposition of a substance in an oxygen free environment, can be used to convert biomass into fuels and other valuable chemicals (de la Rey, 2015, p. 1). Any form of wood can be used, but preference is given to the waste forestry material in the form of sawdust.

This research for generating higher-value products such as crude liquid bio-oil, solid bio-char and combustible producer gas from biomass was conducted at the University of Pretoria, South Africa, by the Chemical Engineering department in partnership with the Paper Manufacturing Association of South Africa (PAMSA), Sappi Southern African (Pty) Ltd and the department of Agriculture in the United States. Three studies were conducted for this process. The first study dealt with the design, modelling and construction of a scalable dual fluidised bed (DFB) reactor system for the pyrolysis of woody biomass (Swart, 2013). The second study dealt with the scalable dual fluidised bed system for fast pyrolysis of woody biomass (Grobler, 2014). The last study was concerned with the energy efficiency in dual fluidised bed fast pyrolysis (de la Rey, 2015).

The two main pyrolysis methods that affect the outcome of the project are the microwave pyrolysis method and the fast pyrolysis method (de la Rey, 2015, p. 1). Research was conducted and it was found that microwave pyrolysis offers great results in producing high quality bio-oil, but fails to completely convert the biomass fed to the process (de la Rey, 2015, p. 1).

On the other hand, the research of the fast pyrolysis method is carried out using a dual fluidised bed reactor where the reactor consists of the combustion fluidised bed (CB),

which is responsible for generating heat and a pyrolysis fluidised bed (PFB), where the biomass gets converted to the desired products (de la Rey, 2015, p. 1). The whole process is called the Combustion Reduction Integrated Pyrolysis System (CRIPS). CRIPS 1 was conducted by Grobler (2014) and is known as the first system. The system included a cyclone which was for bio-char recovery, then followed by a quencher which is for rapid cooling of pyrolysis vapours for the extraction of bio-oil and the non-condensable gases (NCG) (de la Rey, 2015, p. 1). NCG are used as the fuel for CB and the fluidisation medium in the PFB.

The sponsors of this research were interested in seeing this process produce bio-char, which can be used in agriculture and high quality bio-oil, which can be used for heating purposes (de la Rey, 2015, p. 1), but CRIPS 1 was not taking energy efficiency into account and that affected the performance of the system. CRIPS 2 was conducted by de la Rey (2015) and it uses the mass yield approach in order to determine the efficiency of the system, yet still fails to determine the thermal performance and quality of the bio-oil produced.

1.2 Problem Statement and Objectives

Factors such as high energy losses from the fluidised bed and the process as a whole, issues with bio-char recovery and the blockages that mainly occur in the pneumatic feeding of the biomass prevented CRIPS 1 by Grobler (2014) from reaching its best performance and producing the high value products that are desired.

The main objective of this research is to create a system model that consists of a dual fluidised bed and all the relevant components just like the CRIPS 2 system by de la Rey (2015), but now the system must be capable of determining the efficiency of the pyrolysis system while being able to predict the quality of the bio-oil produced from the process.

The system model takes into account all the energy flows that enter and exit the system as well as the mass balance of the system to design, optimize and make alterations to the CRIPS 2 system model with expectations that the factors that reduce the CRIPS 1 performance are reduced or eliminated.

1.3 Method and Scope

The CRIPS system model that is being proposed has been derive from the limitations of the CRIPS 1 model, CRIPS 2 model and the available results of literature study

on the study. Factors such as heat loses, bio-char recovery, bio-oil recovery and the overall efficiency were compared to check performance and validity of the proposed CRIPS model. The proposed model was then optimized to ensure that the maximum possible performance is reached.

It is important to note that the CRIPS process does not produce shaft work and it operates under constant atmospheric pressure conditions (de la Rey, 2015, p. 2). According to de la Rey (2015, p. 2), this simplifies the energy balance of the system to an enthalpy balance approach. Just like in the CRIPS 2 process, the enthalpy was chosen as the reference energy since thermodynamic data available in literature uses enthalpy as the reference point.

2 Literature Review

2.1 Heat Transfer

In order to model and design the CRIPS process appropriately a basic understanding of heat transfer must be comprehended. There are three modes of heat transfer: conduction, convection and radiation. These modes of heat transfer will be discussed below and at the end of this section these modes of heat transfer can be applied to more complex situations.

Conduction occurs between two adjacent surfaces, in thermal contact with each other, where the more energetic atoms transfer energy to the less energetic atoms. According to Cengel and Ghajar (2015, p. 50), one dimensional heat conduction across a plane layer of thickness L is represented as

$$Q_{cond} = \frac{kA}{L}\Delta T \tag{1}$$

where k is the thermal conductivity of the material, A is the area perpendicular to the direction of heat transfer and ΔT is the temperature gradient across the layer.

Heat transfer in the form of convection occurs when a liquid or gas in motion is adjacent to a solid surface. It is a combination of conduction and bulk motion and is expressed as $Newton's\ law\ of\ cooling$ (Cengel and Ghajar, 2015, p. 50) as

$$Q_{conv} = hA_s(T_s - T_\infty) \tag{2}$$

where h represents the convective heat transfer coefficient of fluid in motion, A_s is the solid surface area that the fluid is in contact with, T_s and T_∞ are the surface temperature and ambient temperature respectively.

Radiation is heat transfer that occurs in all directions and does not require a material medium to transfer energy from one substance to another. Energy is emitted in the form of photons as a result of the changes in the electron interactions within the atoms. Radiation emitted from a solid surface to the adjacent gas (air) and is expressed as (Cengel and Ghajar, 2015, p. 50)

$$Q_{rad} = \varepsilon\sigma A_s(T_s^4 - T_{surr}^4) \tag{3}$$

ε is the emissivity of the surface, σ is the *Stefan-Boltzsman constant* where $\sigma = 5.67 \times 10^{-8}$ W/m$^2 K and \mathrm{T}_{surr}$ is the surrounding temperature adjacent to the radiating surface.

2.2 Piping Design

Piping design is a very important consideration for this process as it influences the flowrates and therefore overall energy efficiency. Appropriate assumptions and calculations must be made in order to find the optimal design for piping. Sections of the piping that contain liquid will be regarded as incompressible flow unless they fail the test for incompressible flow, and sections that contain gases or vapours will be regarded as compressible flow. All the theory and equations that are discussed in the subsequent subsections below is according to (Greeff and Skinner, 2000).

2.2.1 Incompressible Flow

For incompressible flow, the standard mechanical energy balance will be used. A number of assumptions and calculations must be considered to determine the optimal piping design for liquids. Flow regime, pipe roughness, pipe material and frictional pressure lost due to pipe sections, control valves and equipment will be discussed below.

Reynolds number is a dimensionless number that is used to to determine the flow regime of the flow and is determined using Equation 4.

$$Re = \frac{Du\rho}{\mu} \tag{4}$$

Table 1 is a summary of the three modes of flow regime:

Table 1: Summary of flow regimes using Reynolds number

Flow Regime	Reynolds number
Laminar	Re $\leq$ 2000
Transitional	2000 $<$ Re $<$ 4000
Turbulent	Re$\geq$ 4000

Frictional factor f' relates to the frictional energy loses due to shear stress of the flow along the pipe wall and therefore they type of flow regime will have an effect. The Colebrook equation can be used to determine f' for laminar, transitional and turbulent flow:

$$\frac{1}{\sqrt{f'}} = -2\log\left(\frac{\epsilon/D}{3.7} + \frac{2.51}{Re\sqrt{f'}}\right) \tag{5}$$

The mechanical energy balance is derived from first law of thermodynamics, where Equation 6 shows the pressure balance (in Pascals) of the piping system

$$\Delta P_{EP} + \Delta P_{EL} + \Delta P_{KE} + \Delta P'_f = \Delta P_a \tag{6}$$

where P_{EP}, ΔP_{EL} and ΔP_{KE} deal with the pressure energy, potential energy and kinetic energy respectively. $\Delta P'_f$ is the frictional pressure losses within the pipeline and will be discussed further below. ΔP_a is the energy added or removed by a fluid mover such as a pump and is normally the unknown term in the MEB to be determined during design. Frictional pressure loss deals with energy losses due to the fluid as well as the components in the pipeline. $\Delta P'_f$ is subdivided as follows:

$$\Delta P'_f = \Delta P_f + \Delta P_{EQ} + \Delta P_{CV} \tag{7}$$

where ΔP_f is the frictional pressure loss due to valves(excluding control valves) and fittings, ΔP_{CV} is the frictional pressure loss due control valves and ΔP_{EQ} is the frictional pressure loss due to equipment and flow instruments.

The Darcy-Weisbach equation is used to determine the frictional energy loss for both laminar and turbulent flow and is represented by Equation 8

$$\Delta P_f = \frac{f'L}{D}\frac{\rho u^2}{2} \tag{8}$$

Elevation pressure difference and endpoint pressure difference are represented by Equation 9 and Equation 10 respectively:

$$\Delta P_{EL} = \rho g(z_2 - z_1) \tag{9}$$

$$\Delta P_{EP} = P_2 - P_1 \tag{10}$$

Kinetic pressure difference is represented as

$$\Delta P_{KE} = \frac{\rho}{2}\left(u_2^2 - u_1^2\right) \tag{11}$$

2.2.2 Compressible Flow

For compressible flow, two models will be considered depending on what design specifications are assumed. Other design considerations that will be done are to check for sonic flow and flow choking. Once the appropriate model has been selected, a modified mechanical energy balance (MEB) corresponding to the selected model will be done to calculate the appropriate unknown parameters. Gases will be treated as ideal gas and in the gases of real gases, a compressibility factor, z, can be included to the equations illustrated below.

Gases or vapours are always considered to be compressible. This means the density and therefore the velocities of the flow will change along a pipeline greatly. However, for design purposes gases or vapors are considered incompressible if

$$\frac{\Delta P_{STV}}{P_1} < 0.1 \tag{12}$$

where fluid density at the upstream of the pipeline is used as the reference point. If Equation 12 is greater than or equal to 0.1, then the flow must be treated as as compressible. Based on the assumptions made,the isothermal or adiabatic models will be used for compressible flow calculations.

Certain thermodynamic principles must be known in order to derive and apply to the two compressible models and their associated equations, however derivation of these models' equation will not be shown. The necessary thermodynamic principles are summarised below:

$$\rho = \frac{MP}{RT} \tag{13}$$

where gas constant $R = 8.314$ J/molK and ρ is calculated under ideal gas conditions.

Relations between R, k and specific heats for ideal gases:

$$C_p - C_v = R \tag{14}$$

$$k = \frac{C_p}{C_v} \tag{15}$$

$$C_p = \frac{kR}{k-1} \tag{16}$$

$$C_v = \frac{R}{k-1} \tag{17}$$

The Mach number is used as a check to determine if sonic flow will occur in a pipeline and is a dimensionless number. For Ma ¡ 1 the flow is subsonic and is the condition that is wanted in piping design. For Ma = 1 and Ma ¿ 1, flow is term as sonic and supersonic flow and should be avoided as it causes shock waves that damages the pipeline. The Mach number is shown as Equation 18:

$$Ma = \frac{u}{c} \tag{18}$$

where c is the sonic velocity and is calculated for an ideal gas:

$$c = \sqrt{\frac{kRT}{M}} = \sqrt{\frac{kP}{\rho}} \tag{19}$$

For long, uninsulated pipelines the isothermal model is usually used. When the flow is considered turbulent, the elevation pressure for the gas in the pipeline is neglected and the frictional pressure loss in the MEB is replaced with Equation 8, then the isothermal model can be used:

$$P_1^2 - P_2^2 = \left(\frac{W}{A}\right)^2 \left(\frac{P_1}{\rho_1}\right) \left(\frac{fL}{D} + 2\ln\left(\frac{P_1}{P_2}\right)\right) \tag{20}$$

The adiabatic model is used typically for short-insulated pipelines where the elevation of the gases or vapor are neglected and there is no fluid movers in-between the two chosen reference points of the pipeline. When all these conditions are meet, Equation 21 can be used

$$\frac{fL}{D} = \frac{k+1}{k} \ln\frac{\rho_2}{\rho_1} + \left(1 - \left(\frac{\rho_2}{\rho_1}\right)^2\right) \left(\frac{k-1}{2k} + P_1\rho_1 \left(\frac{A}{W}\right)^2\right) \tag{21}$$

Equation 20 and Equation 21 are only applicable between two reference points inside a constant-diameter pipe. Analysis must be done incrementally for piping sections of different diameters.

Another important consideration for compressible flow pipe design is to check for flow choking. Flow choking is the maximum length that a pipeline between two reference points for a constant diameter pipe section. Pressure decreases along the pipe, but it is physically not possible for P_2 drop to zero and therefore is a choking of the flow that restricts the mass flowrate.

For isothermal flow, choking occurs when

$$Ma = \frac{1}{\sqrt{k}} \tag{22}$$

and for adiabatic flow choking occurs when

$$Ma = 1 \tag{23}$$

3 Assumptions

- Complete combustion.
- Steady state heat transfer.
- Heat losses through piping is considered negligible.
- Ash component in the flow through the heat exchangers will not be considered for the heat exchangers calculations.
- Heat transfer from the combustion/pyrolysis fluidized bed reactor to the surroundings only occurs in the radial direction.
- Steady state mass flow rates throughout entire system.
- Constant thermal conductivity.
- Effect of radiation at low temperature operations will be checked. However, radiation will be assumed negligible.
- Entry length will be checked to see if it is sufficiently inconsequential and therefore can be neglected. This allows for flow through the heat exchangers to be fully developed.
- Temperatures at the boundary conditions are constant.
- Energy balance will be taken over the entire system for initial calculations using enthalpy data due to simplifying assumptions above.
- CRISPS process is operated at constant atmospheric pressure and no shaft work produced.
- No blockages of biomass and char in the pyrolysis system.
- Pyrolysis Gas recycled back to the combustion fluidised bed is a flue gas.
- No accumulation occurs in the reactor.
- No cracking of secondary gasses will occur.
- Heat transfer coefficients are unknown, but will be calculated using the fluid properties and will be assumed constant.
- All gas phase behaviour is ideal.
- Bio oil vapours are cooled rapidly enough to prevent secondary reactions.

- All separators operate ideally.
- Fouling will not be assumed negligible and will be considered in the heat exchanger calculations.
- Fouling factors are considered as uniform and constant.
- Heat exchangers will be assumed perfectly insulated for initial heat exchanger calculations.
- The thickness of the inner tube of the heat exchanger will be assumed as negligible for the calculation process (a thickness will still be calculated in in later part of the piping design)
- According to Cengel and Ghajar (2015, p. 651), radiation effects within the heat exchanger will be included in the convective heat transfer coefficients of the air and the flue gas.

4 Energy and Mass Flow Analysis

4.1 Mass Flow

4.1.1 Physical Data, Process Considerations and Mass Balance

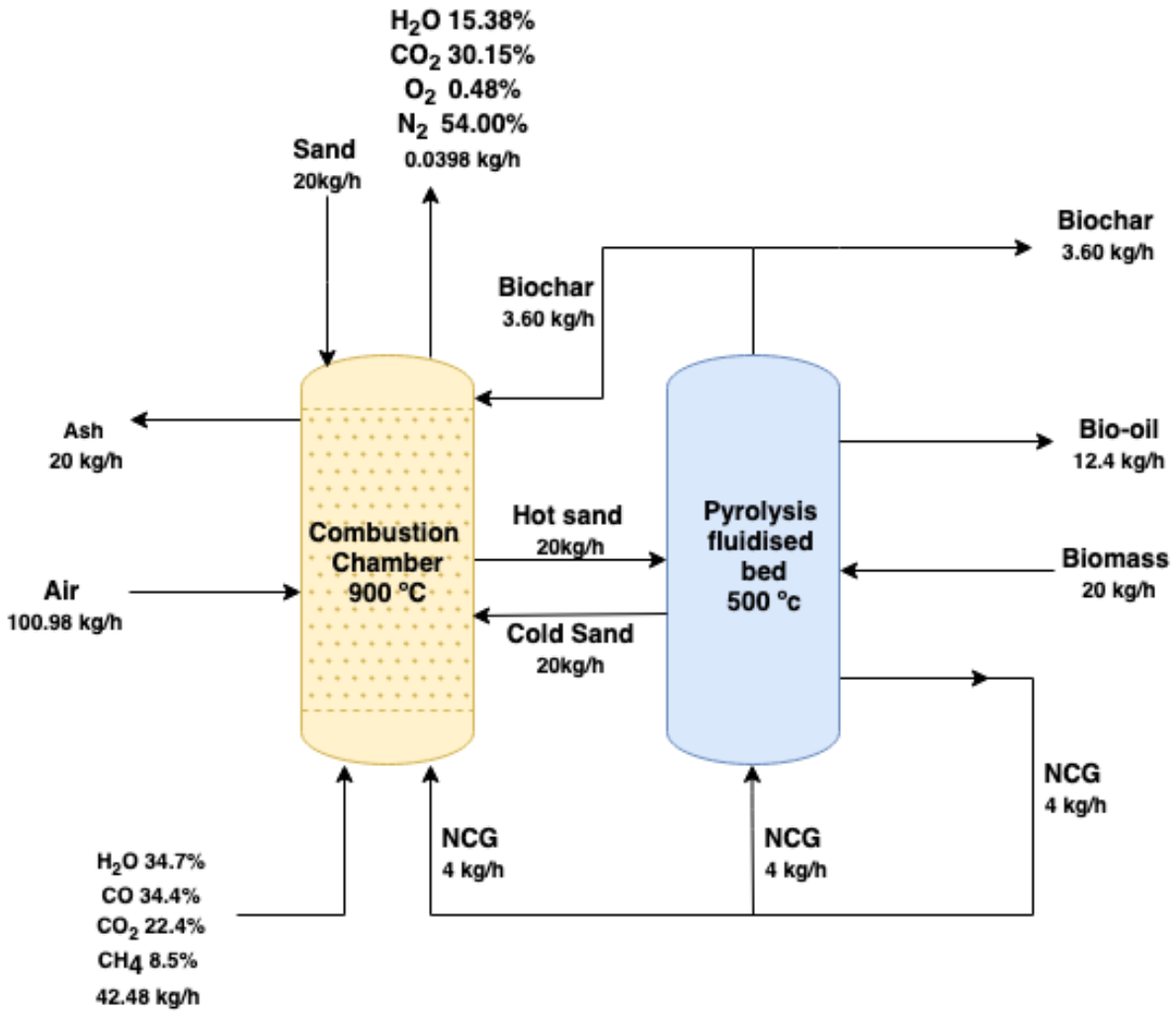

Figure 1: Inflow Process Streams considered for Mass & Energy Balance

Referencing Figure 1, a mass balance over the inflow and outflow streams of the pyrolysis process is done. These calculations will be used in the energy balance over the combustion fluidised bed and all relevant components through the manipulation of constraints considered in this section. The aim in mind is to make sure the mass constraints optimised will provide an energy efficient system while considering both a cost and energy effective heat exchanger option.

Table 2: Mass Based Physical Data

Description	Symbol	Value[a]	Units
Inlet Syn gas Composition			
Water	H_2O	34.7	%
Carbon Monoxide	CO	34.4	%
Carbon Dioxide	CO_2	22.4	%
Methane	CH_4	8.5	%
Sand Feed Rate	S	20	$kg\,h^{-1}$

61

Table 3: Mass Based Constraints

Description	Symbol	Range	Units
Syn Gas Feed Rate	S_{in}	∞	$kg\,h^{-1}$
Air Feed Rate	A_{in}	∞	$kg\,h^{-1}$
Excess Inlet Oxygen	-	$0-5$	%
Biomass Feed Rate	B_{in}	1 - 20	$kg\,h^{-1}$
Sand Recycle Stream	$S_{recycle}$	15 - 30	$kg\,h^{-1}$

$$\dot{m}_{in} = \dot{m}_{out} \tag{24}$$

Where, $\dot{m}_{in}$ is the mass flow rate entering the system and $\dot{m}_{out}$ is the mass flow rate leaving the system. Equation 24 is based on the assumption that there is no accumulation or blockages of any kind within the system.

With the use of Equation 24, the parameters in Table 2 and the constraints in Table 3 (in association with the energy balance in the next section) a mass balance over the system can be done.

4.2 Energy Balance

4.2.1 Physical Data, Process Considerations and Energy Balance

Referencing Figure 1, an energy balance over the inflow and outflow streams of the pyrolysis process is done. The aim in mind is to make sure the energy constraints optimised will provide an energy efficient system while considering both a cost and energy effective heat exchanger option. Please note that through the manipulation of the Exhaust

Temperature (flue gas and ash) and other constraints a favourable set point temperature of the exhaust will be considered in later energy, heat exchanger and piping calculations. Various optimisation testing will be done in an attempt to establish a low exhaust temperature.

Table 4: Energy Based Physical Data

Description	Symbol	Value	Units
Heat Capacity of Water	Cp_W	2.09	$\mathrm{kJ\,kg^{-1}\,K^{-1}}$
Heat Capacity of Carbon Dioxide	Cp_{CO2}	0.84	$\mathrm{kJ\,kg^{-1}\,K^{-1}}$
Heat Capacity of Sand	Cp_S	0.83	$\mathrm{kJ\,kg^{-1}\,K^{-1}}$
Heat Capacity of Ash	Cp_A	1.60	$\mathrm{kJ\,kg^{-1}\,K^{-1}}$
Heat Capacity of Oxygen	Cp_O	0.92	$\mathrm{kJ\,kg^{-1}\,K^{-1}}$
Heat Capacity of Nitrogen	Cp_{N2}	2.09	$\mathrm{kJ\,kg^{-1}\,K^{-1}}$
Higher Heating Value of Syn Gas	HHV_S	6.7	$\mathrm{MJ\,kg^{-1}}$
Higher Heating Value of Biomass	HHV_B	18	$\mathrm{MJ\,kg^{-1}}$
Higher Heating Value of Bio-Oil	HHV_O	6.7	$\mathrm{MJ\,kg^{-1}}$

Table 5: Energy Based Constraints

Description	Symbol	Range	Units
Fluidised Bed Temperature	T_F	700-950	°C
Syn Gas Inlet Temperature	T_{syn}	≤ 50	°C
Outlet Exhaust Temperature	T_E	700-950	°C

$$\dot{Q}_{system} = \dot{Q}_{out} - \dot{Q}_{in} \tag{25}$$

Where,

$$\dot{Q}_{in} = \dot{Q}_{syngas} + \dot{Q}_{biomass} \tag{26}$$

And,

$$\dot{Q}_{out} = \dot{Q}_{Bio-oil} + \dot{Q}_{Bio-char} + \dot{Q}_{exhaust} + \dot{Q}_{loss} \tag{27}$$

With the use of Equation 25, Equation 26, Equation 27, the mass parameters and constraints from the previous section, the parameters in Table 4 and the constraints in Table 5 an energy balance over the system (Figure 1) while aiming to make sure energy requirement of the system ($\dot{Q}_{system}$) is between 45 and 145 MJ/h is done.

To calculate the energy available to the heat exchanger the following process is considered:

$$\dot{Q}_{comb} = \dot{Q}_{fluegas} + \dot{Q}_{Ash} + \dot{Q}_{cond} - \dot{Q}_{syngas} - \dot{Q}_{NCG} - \dot{Q}_{BioChar} \tag{28}$$

Where $\dot{Q}_{syngas}$ is the energy of the inlet syngas, $\dot{Q}_{NCG}$ is the energy of the recycled non condensable gas from the pyrolysis of biomass, $\dot{Q}_{biochar}$ is the energy of the recycled bio-char from the pyrolysis of biomass, $\dot{Q}_{fluegas}$ is the energy of the outlet flue gas from the combustion process, $\dot{Q}_{ash}$ is the energy of the outlet ash from the combustion process and $\dot{Q}_{conduction}$ is the energy transferred from the combustion fluidised bed to the pyrolysis bed through conduction.

$$\dot{Q}_{conduction} = -kA\frac{dt}{dx} \tag{29}$$

To calculate $\dot{Q}_{conduction}$ through the refractories Equation 29 will be used.

According to de la Rey (2015, p. 39) an assumption can be made that 56% of $\dot{Q}_{combustion}$ is transferred to the heat exchanger 35% of $\dot{Q}_{combustion}$ is transfer through the sand circulation and the rest is thought to be lost energy. With this in mind the energy available to the heat exchanger can now be calculated.

Apart from the stipulated energy requirement range, a second check to see if all the energy requirements of the system are in place would be to be make sure that the energy required for pyrolysis (1.4 MJ/kg biomass consumed) is met by using Equation 30.

$$\dot{Q}_{pyro} = \dot{Q}_{Bio-char} + \dot{Q}_{Bio-oil} + \dot{Q}_{NCG} + \dot{Q}_{loss} - \dot{Q}_{cond} - (0.35)\dot{Q}_{comb} - \dot{Q}_{NCG_R} \tag{30}$$

Where, $\dot{Q}_{Bio-char}$ is the energy leaving the pyrolysis through the bio-char, $\dot{Q}_{Bio-oil}$ is the energy leaving the pyrolysis through the bio-oil, $\dot{Q}_{NCG}$ is the energy leaving the pyrolysis through the non-condensable gas, $\dot{Q}_{loss}$ is the energy loss from the pyrolysis bed to the environment, $\dot{Q}_{conduction}$ is the energy transferred to the pyrolysis bed from the combustion fluidised bed through conduction, $0.35(\dot{Q}_{combustion})$ is the 35% of $\dot{Q}_{combustion}$ transferred through the sand circulation, $\dot{Q}_{NCG_R}$ is the energy transferred through the recycle of the non condensable gas.

4.3 Summary of Results: Mass and Energy Balance

The table below shows a summary of the results obtained from the mass and energy balance equations through the manipulation of the constraints mentioned above.

Table 6: Results

Desciption	Chosen Value	Units
Syn Gas Inlet Temperature	323.15	K
Syn Gas Inlet Mass	41	$\mathrm{kg\,h^{-1}}$
Air Fed To the System	100.97	$\mathrm{kg\,h^{-1}}$
Sand Fed to the System	20	Kg
Syn Gas Inlet Flow Rate	1.5	$\mathrm{kg\,h^{-1}}$
%Excess O2	3	%
Biomass Feed Rate	20	$\mathrm{kg\,h^{-1}}$
Sand Recycle	20	$\mathrm{kg\,h^{-1}}$
Pyrolysis Bed Temperature	773.15	K
Combustion Fluidised Bed Temperature	1173.15	K
Bio Char recycled to Combustion Fluidised Bed	50	%
NCG Recycled back to Pyrolysis Bed	50	%
Flue Gas From Combustion Fluidised Bed	143	$\mathrm{kg\,h^{-1}}$
NCG from Pyrolysis Process	4	$\mathrm{kg\,h^{-1}}$
Bio-Char from the Pyrolysis Process	3.6	$\mathrm{kg\,h^{-1}}$
Bio-Oil from the Pyrolysis Process	12.4	$\mathrm{kg\,h^{-1}}$
Ash Out from combustion Process	24	$\mathrm{kg\,h^{-1}}$
Inlet Air Temperature	20	°C
Outlet Air Temperature	677	°C
Inlet Flue Gas Temperature	900	°C
Outlet Flue Gas Temperature	570	°C
Energy Required By the System	70.09	$\mathrm{MJ\,h^{-1}}$

The energy requirement of the current systems design is 70 $\mathrm{MJ\,h^{-1}}$ which is between the stipulated energy requirement of 45 and 145 $\mathrm{MJ\,h^{-1}}$.

5 Heat Exchanger and Piping Design

5.1 Heat Exchanger Calculation Process

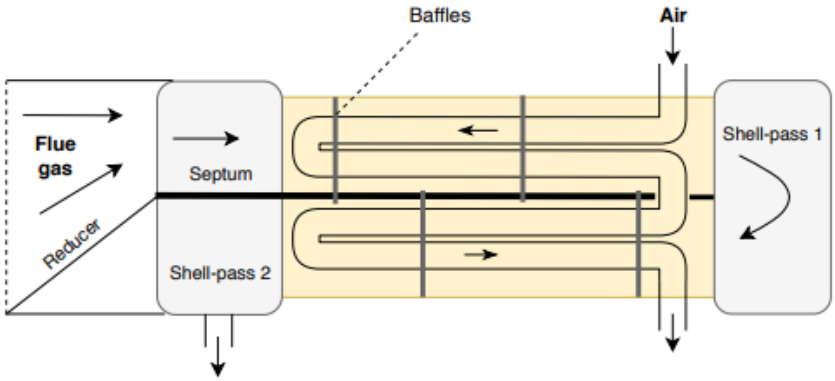

Figure 2: Heat Exchanger Configuration

Figure 2 represents the heat exchanger of which the calculations in this section will be based on (2 Pass Shell and Tube).

With the energy available to the heat exchanger calculated, its outlet exhaust (flue gas and ash) optimised the heat exchanger design process will be undertaken using the Effectiveness-NTU method.

With inlet air temperature of 20 °C , an outlet air temperature of 828 °C, an inlet exhaust (flue gas and ash) temperature of 900 °C (based on the assumption that the exhaust from the combustion process enters the heat exchanger at the same temperature as the Combustion Fluidised Bed) and an outlet exhaust temperature of 548 °C the required heat transfer rate of the heat exchanger for its operation can be calculated.

$$\dot{Q}_{required} = (\dot{m}Cp\Delta T)_{Air} = (\dot{m}Cp\Delta T)_{Exhaust} \tag{31}$$

Where $\dot{Q}_{required}$ is the energy transfer required for the operation of the heat exchanger based on both the air stream fluid and exhaust stream fluid (Flue gas and ash).

From the Energy Balance Section the energy available to the heat exchanger was 125 MJ/h (34.72 kW) and by using Equation 31 on the exhaust stream and the air stream the, energy required by the heat exchanger to operate is 66 MJ/h (18.53 kW). $\dot{Q}_{required} \leq \dot{Q}_{available}$ meaning the that there is more than enough energy available to the heat exchanger.

As a starting point of sizing the shell and tube heat exchanger an approximate estimate of the overall heat transfer coefficient of 15 $\mathrm{W\,m^{-1}\,K}$. This value is suppose to range between 10-40 $\mathrm{W\,m^{-1}\,K}$ according to Cengel and Ghajar (2015).

The favourable configuration of the heat exchanger would be to have the the (flue gas and ash) on the tube side since the fluid is more likely to foul. This would make the cleaning of the heat exchanger much more tolerable seeing as the air has no potential to cause fouling. However, to make the flow of the flue gas into the heat exchanger more practical the flue gas will flow in the tube side and the air will flow in the shell side. This is in order to avoid the impracticality of having a fluid mover, reducer and flow splitting device inside the combustion zone, which would be costly and these apparatus would experience fouling of a similar degree and require extensive maintenance due to the high temperature.

The heat exchanger was to be sized to fit into the combustion fluidised bed which has a diameter of 0.250 m, however it was later resized by cutting the refractory and fixing the heat exchanger directly onto it. More information on this design choice is provided in the optimisation section.

The sizing procedure is as follows:

$$\dot{Q}_{max} = C_{min}(Th_{in} - Tc_{in}) \tag{32}$$

Where, $\dot{Q}_{max}$ is the maximum possible heat transfer rate, C_{min} is the smaller value of C_h and C_c. Take note that $C_h = \dot{m}Cp_{ph}$ and $C_c = \dot{m}Cp_{pc}$. Th_{in} is the in hot stream temperature and Tc_{in} is the inlet cold stream temperature.

$$\dot{Q}_{actual} = (\dot{m}Cp\Delta T)_{Air} = (\dot{m}Cp\Delta T)_{Exhaust} \tag{33}$$

Where, $\dot{Q}_{actual}$ is the actual heat transfer rate which is calculated using the same process as Equation 31.

With a calculated maximum heat transfer rate and a calculated actual heat transfer rate the heat transfer effectiveness can be calculated using Equation 34

$$\epsilon = \frac{\dot{Q}_{actual}}{\dot{Q}_{max}} \tag{34}$$

$$c = \frac{C_{min}}{C_{max}} \tag{35}$$

Where c is the capacity ratio, C_{min} is the smaller value of C_h and C_c and C_{max} is the larger value of C_h and C_c

With a calculated c value from Equation 35 and a calculated ϵ from Equation 34 the NTU value can be read of from a graph found in Cengel and Ghajar (2015, p. 676).

$$A_s = \frac{NTUC_{min}}{U} \tag{36}$$

Where NTU is the number of transfer units read off from the graph, U is the estimated overall heat transfer coefficient and A_s is the area estimate of the Shell and Tube Heat Exchanger.

With an estimated Area, the number of tubes and length of tubes can be calculated using Equation 37

$$A_s = N_t(\pi D_i)L_t \tag{37}$$

Where, A_s is the area of the heat exchanger, D_i is the tube diameter of the exhaust in this case, L_t is the tube length.

Equation 37 will be used to calculate an iterated area value until this area matches the estimated area of the heat exchanger calculated in Equation 36.

To iterate Equation 37 the following tube diameter constraints were considered; $\frac{1}{4}$, $\frac{3}{8}$, $\frac{1}{2}$, $\frac{1}{2}$, $\frac{5}{8}$, $\frac{3}{4}$, 1, 1.25, 1.50 inch. The lengths of the tube to be optimised is 8, 10, 12, 16, 20 inch and the number of tubes are in multiples of 4 to accommodate for the 25 shell pass heat exchanger option used and the long tube length of that would have to fit in the vessel.

The above idea can also be viewed as an optimisation process.

$$V_{flue} = \frac{m_{flue}}{\rho(\frac{\pi}{4}D_o^2 - \rho\frac{\pi}{4}D_i^2 n_{tube})} \tag{38}$$

Where, V_{flue} is the calculated velocity of the flue gas, m_{flue} is the mass flow rate of the flue gas and D_i is the diameter of the tube, D_o is the outer diameter and n_tube is the number of tubes the heat exchanger has.

$$Re_{flue} = \frac{V_{flue} D_i}{\mu} \tag{39}$$

Where Re_{flue} is the flue gas Reynolds number, V_{flue} is the calculated flue gas velocity from Equation 38.

With a Reynolds flue gas value calculated a nusselt equation is specified in this case the nusselt equation for the specified Reynolds number is:

$$Nu_{flue} = 0.023 Re_{flue}^{0.8} Pr_{flue}^{0.4} \tag{40}$$

Where Nu_{flue} is the calculated nusselt number of the flue gas and Pr_{flue} is the Prandtl number of the flue gas from literature.

$$h_{flue} = \frac{k_{flue} Nu_{flue} Pr_{flue}^{0.4}}{D_i} \tag{41}$$

Where h_{flue} is the convective heat transfer of the flue gas.

The next step would be to calculate the convective heat transfer coefficient of the air using the following steps:

The velocity of the air V_air will be kept at 10 $\mathrm{m\,s^{-1}}$ by using a blower and a control valve for the inlet pipe of the air.

$$Re_{air} = \frac{V_{air} D_i}{\mu} \tag{42}$$

Where Re_{air} is the air Reynolds number, V_{air} is configured air velocity through the tubes of the heat exchanger and μ is the kinematic viscosity of the fluid.

The Nusselt equation for the specified Reynolds number is:

$$Nu_{air} = 0.023 Re_{air}^{0.8} Pr_{air}^{0.4} \tag{43}$$

Where Nu_{air} is the calculated nusselt number of the air and Pr_{air} is the Prandtl number of the air from literature.

$$h_{air} = \frac{k_{air} Nu_{air} Pr_{air}^{0.4}}{D_i} \tag{44}$$

Where h_{air} is the convective heat transfer of air.

$$U = \frac{1}{\frac{1}{h_{air}} + R_{f,i} + R_{f,o} + \frac{1}{h_{flue}}} \tag{45}$$

Where U is the calculated overall heat transfer coefficient of the heat exchanger, $R_{f,o}$ is the the fouling factor of the shell surface and $R_{f,i}$ is the fouling factor of the tube surface.

With a calculated U value the the energy the shell and tube heat exchanger actually uses can be recalculated by reusing the NTU Method discussed above.

By referring to the results section of the heat exchanger it can be seen that the Reynolds number is above 10000 and the Prandtl number is between 0.7 and 160, which is why Equation 40 and Equation 43 to calculate the Nusselt number. D_o which is the inner diameter of the shell side is optimised by using the the combustion zone diameter, the additional space provided by the refractory and the assumption that some of the available space will be used to mechanically fix the heat exchanger to the refractory. The area of the shell side as well as the bundle diameter were also be compared to the area of the tube side to make sure that the shell is able to accommodate the tube bundle of the heat exchanger. Furthermore, flow choking was also investigated and found to be unproblematic.

5.2 Fins

By considering the values from the results of the heat exchanger design in the next subsection it is clear that the convective heat transfer coefficient of the tube side is drastically lower than that of the shell side.

A solution to this is to add fins to the tube side of the heat exchanger. This will increase the surface area and thus enhance heat transfer. After looking at various fin options, the best choice seems be to have a fin design that has helical fins depressed into the tube. It was decided to investigate the feasiblity of this idea by using disc shaped radial fins as an estimate due to ease of calculation.

The process for calculating the fins is as follows;

The fist step after optimising the best fin dimensions will be to calculate the number of fins that would be installed on one tube.

$$A_{nofin} = \pi D_i L_{tube} \tag{46}$$

Where, A_{nofin} is the area on the one tube with no fins, L_{tube} is the length of one tube within the heat exchanger.

$$Q_{nofin} = A_{nofin} h_{flue} (T_{b,flue} - T_{b,air}) \tag{47}$$

Where Q_{nofin} the heat transfer rate with no fins, h_{flue} is the convective heat transfer coefficient of flue in the shell side of the heat exchanger. h_flue is calculated using Equation 41. $T_{b,flue}$ is the bulk temperature of the flue gas which is the calculated average between the inlet and outlet temperature of the tube. $T_{b,air}$ is the bulk temperature of air which is the calculated average between the inlet and outlet air temperature of the shell side.

Although the fins in this design will be helical they will be approximated as circular fins of a rectangular profile as an attempt to simplify the calculation process.

$$A_{fin} = 2\pi (r_{2,c}^2 - r_1) \tag{48}$$

Where, A_{fin} is the area of the fin, $r_{2,c}$ is calculated using Equation 49which is based on r_2 and t which is based on the configuration in Figure **??**

$$r_{2,c} = r_2 + \frac{t}{2} \tag{49}$$

$$Q_{fin} = A_{fin} h_{air} (T_{b,flue} - T_{b,air}) n_{fin} \tag{50}$$

Where Q_{fin} is the heat transfer rate with fin around one tube of the heat exchanger and n_{fin} is the number of tubes found on one tube

$$e = \frac{Q_{fin}}{Q_{no,fin}} \tag{51}$$

Where e is the effectiveness of the heat exchanger based on the heat transfer rate with and without the fin.

With an effectiveness number value either below or above 1, a decision will be made to see how having fins will actually improve the heat transfer from the tube side to the shell side of the heat exchanger.

$$A = A_{fin} n_{fin} - A_{unfin} \tag{52}$$

Where A is the new area of the tube which includes the fins, A_{unfin} is the area of the tube with no fins.

If having fins on the tube side is seen as feasible a new area will be calculated using Equation 52.

$$n_t ubes = \frac{A}{\pi D_i L_{tube}} \tag{53}$$

Where n_{tubes} is the new number of tubes bases on the new calculated area from Equation 52 based on the same tube length (L_{tube}) and outer tube diameter (D_o) as before.

The final decision will be discussed in the optimisation section.

5.3 Heat Exchanger Energy Loss

Heat is transferred from a hot fluid to a cold fluid, using the idea the bulk temperature of the flue gas in the shell side is less than the constant temperature of the pyrolysis bed of 500 °C heat will flow from the shell side of the heat exchanger to the pyrolysis bed. This will cause a further drop in the the outlet temperature of the heat exchanger and the energy will be recycled into the pyrolysis zone.

$$Q_{conduction} = -k \frac{dT}{dx} \tag{54}$$

Where, $Q_{conduction}$ is the conduction through the shell of the heat exchanger, dT is the temperature difference between the bulk mean temperature of the flue gas and the pyrolysis bed temperature of 500 °C and dx is the conduction path of the heat transfer.

$$Q_{convection} = h_p A_s \Delta T \tag{55}$$

Where, $Q_{convection}$ is the heat convective heat transfer between the shell of the heat exchanger and the the pyrolysis bed, h_p is the convective heat transfer of the pyrolysis bed, Δ T is the temperature difference between the bulk mean temperature of the flue gas and the pyrolysis bed temperature.

$$Q_{r,s} = \epsilon_c \sigma (T_{b,f}^4 - T_{b,a}^4) \tag{56}$$

Where $Q_{r,s}$ is the radiation from the tube surface to the shell surface of the heat exchanger, ϵ_c is the emissivity of the copper material, σ is the Boltzmann Constant, $T_{b,f}$ is the bulk temperature of the flue gas in the shell and $T_{b,a}$ is the bulk temperature of the air in the tubes of the heat exchanger.

$$Q_{r,t} = \epsilon_s \sigma (T_{b,f}^4 - T_{b,a}^4) \tag{57}$$

Where $Q_{r,t}$ is the radiation from the shell surface to the tube surface of the heat exchanger, ϵ_s is the emissivity of the stainless steel material, σ is the Boltzmann Constant, $T_{b,f}$ is the bulk temperature of the flue gas in the shell and $T_{b,a}$ is the bulk temperature of the air in the tubes of the heat exchanger.

Considering Equation 56 and Equation 57 the ϵ_c is 0.65 and the ϵ_s is 0.15 at the respective bulk temperatures of the tube side and shell side of the heat exchanger. Because of this $Q_{r,s}$ will be larger than $Q_{r,c}$, meaning more radiation is happening from the tube side to the shell side of the heat which will add on to the heat exchanger loss calculation.

Assuming a steady state operation of the heat exchanger $Q_{conduction} = Q_{convection}$

That being said energy loss from the heat exchanger through the shell can now be calculated.

$$Q_{loss} = Q_{conduction} + Q_{r,s} - Q_{r,c} \tag{58}$$

Where Q_{loss} is the energy loss of the heat exchanger.

Using the above equation the outlet flue gas temperature of the heat exchanger will be 548 °C as opposed to the original value of 570 °C (obtained from $Q_{required}$) and the Qloss of the heat exchanger is 0.68 kW.

The outlet temperature of the heat exchanger is acceptable since this temperature is above the condensable temperature ranges of the heat exchanger.

5.4 Baffles

Baffles are flow directing panels that are installed in industrial process vessels such as shell and tube heat exchangers. They form an important integrated part of the heat exchanger design. Baffles are usually installed in the shell side of the shell and tube heat exchanger to support tube bundles and to direct the fluid in the shell side. Some of the advantages of baffles are to prevent sagging by holding the tubes in position inside the heat exchanger and direct the fluid in the shell side of the heat exchanger over the tubes, as a result this increases the fluid velocity and the heat transfer co-efficient.

According to Sinnott et al. (2005, p. 658) baffles spaced optimally for flow are between 0.3 to 0.5 times the shell diameter. The spacing has been chosen to be 0.5 times the outer diameter, which gives enough support for the tubes without severely impeding the flow or increasing the pressure drop excessively.

This gives us 8.6 baffles, so we will use 9 baffles instead, with a spacing of 67 mm.

5.5 Heat Exchanger Pitch Selection

Pitch refers to the nature and magnitude of the spacing between pipes. It is instrumental in ensuring proper heat transfer and flow through the shell. (Sinnott et al., 2005, p. 670) states that the square arrangement gives us the best cleaning ability. This is important because we have selected the flue gas as the shell side fluid. This was due to the impracticality of directing the flue gas to flow through the tubes without building up pressure in the bed, which will interfere with the fluidisation of the bed.

The pitch has been chosen as 28 mm based on the heuristic from (Sinnott et al., 2005, p. 670) that the pitch should be approximately 1.25 times the tube diameter. Figure 3 indicates a rough visualisation of the selected pitch.

5.6 Material of Construction

Copper and Stainless steel are the materials used to construct the heat exchanger because of their chemical properties. The tubes are designed using copper, while the shell is designed using stainless steel.

The properties of copper dictate that it a good thermal conductor of heat. Pure copper typically has a thermal conductivity of approximately 386.00 W/m.K at a temperature

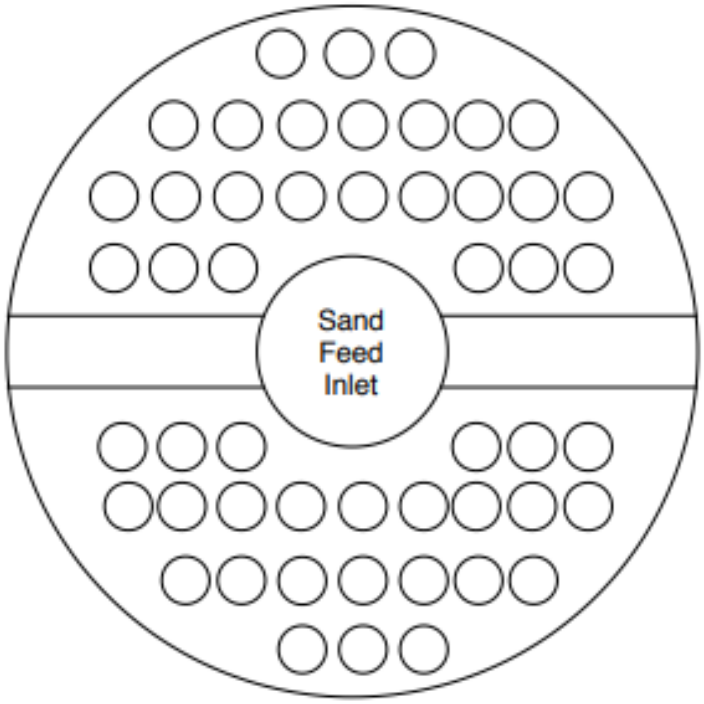

Figure 3: Heat exchanger configuration front view

of 20 °C. As a result, this makes copper one of the most conductive metals. Copper also has a relatively low specific heat which is about 0.385 J/g.°C which supports its use in heat exchangers. The melting point of copper 1085C, which implies it will be able to handle high temperature values of the fluid that flows through it. Besides copper having a disadvantage of developing verdigris, which is a layer of patina that forms on copper due to atmospheric oxidation over time, copper has an exceptional resistance to corrosion and has ductile failure modes, which are preferred over the brittle failure modes of materials such as high temperature resistant ceramics.

On the other-hand, stainless steel has a thermal conductivity of about 14.4 W/m.K at 20 °C, a specific heat capacity value of 0.502 J/g.°C, a melting point of 1510 °C and it has a similar resistance to corrosion as copper. The low thermal conductivity is good for minimizing the heat lost from the shell to the environment. The high melting point is able to accommodate the high temperature products in the process. Stainless steel is also easy to work with and weld, which is advantageous because it will be fixed to the reactor shell.

5.7 Heat Exchanger Design Results

Table 7: Heat Exchanger Results

Heat Exchanger Type	Shell and Tube	Units	
Configuration	2 Shell Pass	-	
Area (No Fins)	3.41	m^2	
Available Energy	34.72	kW	
Required Energy	18.53	kW	
Heat Transfer (No Fins)	23.01	kW	
Material	Copper and Stainless Steel	-	
Side	**Tube Side**	**Shell Side**	
Fluid Circulated	Air	Flue Gas	
Physical Properties			
Density	0.	0.42	kg/m^3
Thermal Conductivity	0.05352	0.06684	$W\,m^{-1}\,K$
Kinematic Viscosity	7.16×10	0.000107	m^2/s
Prandtl number	0.6969	0.7242	
Fouling Factor	0.000	0.001	
U Estimate	1		
Calculated U Value	17.8		
Operating Condition			
Temperature in	2	90	°C
Temperature out	67	54	°C
Calculated Values			
Velocity	10 11.78	$m\,s^{-1}$	
Reynolds Number	19567	15290	
Nusselt Number	54	45	
Prandtl Number	0.69692	0.724	
Heat Transfer Coefficient	20.6	189.47	W/m^2K

Table 8: Heat Exchanger Results

Tubes		
Number of Tubes	28	
Inner Diameter	0.0254	m
Outer Diameter	0.0294	m
Total Bundle Area	0.01419	m^2
Material	Copper	
Shell Side		
Outer Diameter	0.14	m
Total Area	0.02	m^2
Material	Stainless Steel	
Fins		
Inner Radius	0.0132	m
Outer Radius	0.0152	m
Thickness	0.001	m
Length	0.0045	m
Spacing Between Fins	0.003	m
Area of one Fin	0.000453	m^2
Number of Fins	30	
Heat Exchanger Area	3.65	m^2
Calculated Q (With Fins)	23.21	kW
Effectiveness	1.896	
Energy Loss	0.68	kW

From the results above it can be deduced that it would not be feasible to have fins of this length, since the number of tubes and energy requirement of the heat exchanger would increase, however using more space for fins would notbe practical considering the space limitations present in the bed.

Without considering fins, the energy used by the heat exchanger for its operation is 23.01 kW which is above the 18.53 kW required energy of the heat exchanger and within the range of available energy that the flue gas can supply to the heat exchanger which is 34.72 kW.

6 Piping System Design

This section contains only the piping design aspects that are not directly involved in the heat exchanger sizing process. The preceding section, as the reader may have noticed, includes the piping checks regarding Reynolds number, Nusselt number, fluid velocity and flow choking for both the shell and tube side.

6.1 Wall thickness

Selection of wall thickness for piping is critical to prevent failures due to stresses that exceed the yield strength of the piping material according to Greeff and Skinner (2000, p. 77). Equation 59 will be used to calculate the wall thickness of the shell and tube piping.

$$t_{min} = M\left(\frac{Pd_o}{2(SE+PY)} + C\right) \tag{59}$$

Firstly, a frictional factor had to be determined for the flue gas and air flowing through the shell and tube piping. Based on their Reynolds numbers, the two flows are turbulent and Equation 8 was used to determine their frictional factors.

Table 9: Input values for shell and tube thickness calculation

Symbol	Description	Shell Value[a]	Tube Value[a]	Units
P_{max}	Maximum system pressure	28	50	kPa
S	Allowable stress	205×10^3	40×10^3	kPa
M	Fabrication tolerance factor	1.125	1.125	-
E	Joint quality factor	1	1	-
d_o	Outer diameter	14	1.6	cm
Y	Toughness of material factor	0.5	0.5	-
C	Sum of allowances for corrosion, erosion	0.1	0.1	cm

[a] (Perry and Green, 2008)

Then the values from Table 9 were inserted into Equation 59. The results were a minimum wall thickness for the shell as 3 mm and for the tube as 2 mm.

6.2 Calculation of pressure drop through the heat exchanger

Pressure drops for the shell and tube were calculated using values from Table 10 entered into Equation 8. The equivalent length, Lr, was determined using Equations 60 of the shell and tube. Thereafter, the equivalent lengths were added with pipe section lengths to get the total lengths of the piping.

Table 10: Input values for shell and tube pressure drop calculations

Symbol	Description	Tube Value	Shell Value	Units
t_{tube}	Wall thickness	2[a]	3[a]	mm
Re	Reynolds number	19 566[a]	15 290 [a]	15290[a] -
D	Inner pipe diameter	0.016[a]	0.14[a]	m
f'	Frictional factor	0.0272[a]	0.0297[a]	-
u_{air}	Air flow velocity	10[a]	11.8[a]	$\mathrm{m\,s^{-1}}$
K_r	K-value	3.982[b]	1.9198[b] -	
L_r	Equivalent length of the restriction	2.342[b]	9.05[b]	m
L_P	Pipe section length	2.4384[a]	1.2192[a]	m
L_r	Global equivalent length	4.784[a]	10.269[a]	m

[a] Calculated
[b] (Greeff and Skinner, 2000, pp. 29, C3-C5)

$$Lr = \frac{K_r D}{f'} \tag{60}$$

As a result, it was determined that the pressure drop for the tube was calculated to be 0.5668 kPa and for the shell to be 0.08367 kPa. It should also be noted that baffle allowances had to be added to the pressure drop on the shell side due to the fact that baffles impede flow somewhat.

6.3 Delivery line and Blower

The delivery line for the air was selected based on the piping design equations in the theory section of this document. The blower was sized using a manufacturers automated sizing system. This sizing resulted in the HP2 Series- 6B blower being selected, which is able to handle the specified pressure delivery. The information and sizing criteria pertaining to this blower is according to CincinnatiFan (2019) which has an interactive sizing web page.

The line was sized with a thickness of 3 mm and a diameter of 0.14 m using the standard piping design method outlined in the literature review.

7 Design Optimisation, Constraints and Sensitivity Considerations

7.1 General Approach

This optimisation section will detail the methods used for optimisation. The first consideration will be the energy balance, following which the heat exchanger sizing calculations and practical optimisations will be considered.

Typically, practical optimisations are more likely to be stated as design choices but have been added here so that the reader may have a full view of what has been added to the basic heat exchanger design. The actual calculation methodologies will be listed in the section relevant to the item in question and the final values will all be collated in a table, both for ease of reading.

Sensitivity ties in to optimisation in that optimisation specifies a set point and primary objectives deviating from these set points due to parameter changes is indicative of sensitivity. As such, these sections were grouped together.

7.2 Energy and Mass Balance

The energy balance is optimised to operate at maximum biomass throughput, while varying all other variable flowrates in the given ranges to achieve the required energy values. From these combinations, the best one for the heat exchanger design was chosen.

7.3 Temperature Difference Selection

It is known that the flue gas should not be at a temperature which is low enough for any of its constituents to condense. This is the basis upon which the temperature difference was selected. An allowance was also added to the minimum temperature in order to ensure that the dynamics of operation would not result in condensation.

7.4 Shell and Tube side fluid specification

It is common practice to use the tubes to house the more corrosive fluid, as it reduces the effects of corrosion and is easier to clean. However, it is impractical to have the flue gas directed into the tubes with sufficient linear velocity without building up excessive pressure in the bed, which will be problematic due to the fact that the sand is fed through the heat exchanger. Insertion of a blower or fan of some sort was considered, but due to the space constraints and the limitations of operation at high temperature this was found to be uneconomical and impractical. The flue gas was then chosen to be the shell side fluid and the air was chosen to be the tube side fluid. This choice is further supported by the changes made in the following subsection.

7.5 Heat Exchanger Dimensions and Placement

Since space in the combustion chamber is limited, it was suggested to cut the refractory and have the heat exchanger sit on top of it. This will allow the pyrolysis bed to come into contact with the outside of the heat exchanger, thus no insulation is necessary around the heat exchanger as the heat lost from the fluid in the shell is effectively recycled, thus our heat exchanger heats the pyrolysis zone as well, albeit to a limited degree. This was implemented into the design.

Since the flow in both the combustion and pyrolysis zone is longitudinal, there will not be significant strain on the heat exchanger. Furthermore, the shell can be welded onto the outer reactor shell, which further supports the choice of stainless steel as the shell material.

The heat exchanger was placed longitudinally to achieve better length along the tubes. It is also a better orientation due to the fact that the combustion zone is cylindrical. The tubes are also longitudinally arranged to avoid excessive pressure drop.

The height of the heat exchanger is limited by how much space is available within the combustion zone. Since the reactor is 1.6 m in length, we decided that the heat exchanger length should be limited to 0.6 m. Standard tube lengths were used, and bent to approximately 0.6 m.

7.6 Fins

The use of fins to increase surface area was investigated. However, the additional pitch required for this to be useful would not have been feasible with the space available, so although we had done all the required calculations, we were forced to abandon the usage of fins.

7.7 Heat Losses

The heat losses from the outer surface of the heat exchanger will flow into the pyrolysis bed, which allows better heating in the pyrolysis chamber as well as cooling of the flue gas, this means that no heat is wasted from the heat exchanger. The losses were calculated using a steady conduction model through the shell.

7.8 Sand Feed Channel

Since the reactor needs to periodically be charged with sand, we have a central hole included in the heat exchanger, which will be covered by a plate to eliminate heat loss when not in use.

7.9 Process parameter variations

Since the heat exchanger is inside the combustion bed, ambient conditions will not directly affect it and the control measures for maintaining the temperatures of the pyrolysis and combustion bed will be sufficient.

Varying flowrates do affect the linear velocity of the flue gas within the shell, but since the air is forced through the tubes by a blower, the blower speed can be adjusted to ensure heat transfer is maintained. For this to be possible, the tubes were sized near the highest possible flowrate.

7.10 Cleaning and maintenance

Since the shell side fluid will likely deposit ash and cause corrosion, the square pitch was used, which makes for easier cleaning according to (Sinnott et al., 2005, p. 685). A floating header was considered but will have to be specially fabricated for this application due to the sand feed hole, and was thus abandoned in this design due to that fact that it is a pilot plant and should not incur excessive cost.

8 Conclusions and recommendations

The main constraints in this design are the space available for the heat exchanger and the fact that sand needs to be loaded into the bed. These constraints limit the amount of heat transfer that is possible. Cutting the refractory is a good way to alleviate the former issues, however the latter is more difficult to address. Measures to work around it were not implemented in this design but we suggest the usage of an alternative feed location such as blowing it into the bed with the air feed. The extremely high temperatures are also problematic for design, which is why the design had to prioritise practicality by using the shell side for the hot fluid.

It would also be wise to evaluate the feasibility of a heat exchanger that is not within the reactor shell if one were building a new plant of this nature. On the current plant the cost and inconvenience outweighs the benefit as it is a small scale operation and is not continuously operated.

The flowrates and constraints that this document are based on were estimated ranges and more specific data will yield better design optimisation. The degree to which mechanical changes to the plant itself were possible was not explicitly stipulated therefore the design was created under the assumption that changes should be as cheap as possible and cause minimal interference. As such, values reported here should be reevaluated before being implemented unless the same flowrates and temperatures are being used.

It is further recommended that the synthesis gas inlet temperature should be monitored and an additional heat exchanger should be used to heat it up if feasible.

Overall, this design takes advantage of cost effectiveness and the space available by cutting into the refractory and thereby limiting energy wastage. It will help heat up the pyrolysis zone as well as preheat the air feed thereby saving energy. Furthermore, this design is not costly to implement, which is usually quite an important factor in pilot plants.

References

Cengel, YA and AJ Ghajar (2015). *Heat and Mass Transfer: Fundamentals and Applications*. 5th edition. New York: McGraw-Hill.

CincinnatiFan (2019). *High pressure blowers*. URL: `https://www.cincinnatifan.com/catalogs/HPII-1104-internet.pdf` (visited on 10/12/2019).

de la Rey, J (2015). "Energy efficiency in dual fluidised bed fast pyrolysis". In: *University of Pretoria* November.

Greeff, IL and W Skinner (2000). *Piping System Design*. University of Pretoria: Department of Chemical Engineering.

Grobler, ABL (2014). "Scalable dual fluidised bed system for fast pyrolysis of woody biomass". In: *University of Pretoria*.

Perry, RH and D Green (2008). *Perry's Chemical Engineer's Handbook*. 8th edition. Internaltional: McGraw-Hill.

Sinnott, RK, JM Coulson, and JF Richardson (2005). *Coulson Richardson's chemical engineering. Vol.6, Chemical engineering design*. 4th edition. Oxford: Elsevier Butterworth-Heinemann.

Swart, SD (2013). "Design, modelling and construction of a scalable dual fluidised bed reactor for the pyrolysis of biomass". In: *University of Pretoria*.

A Process flow diagram

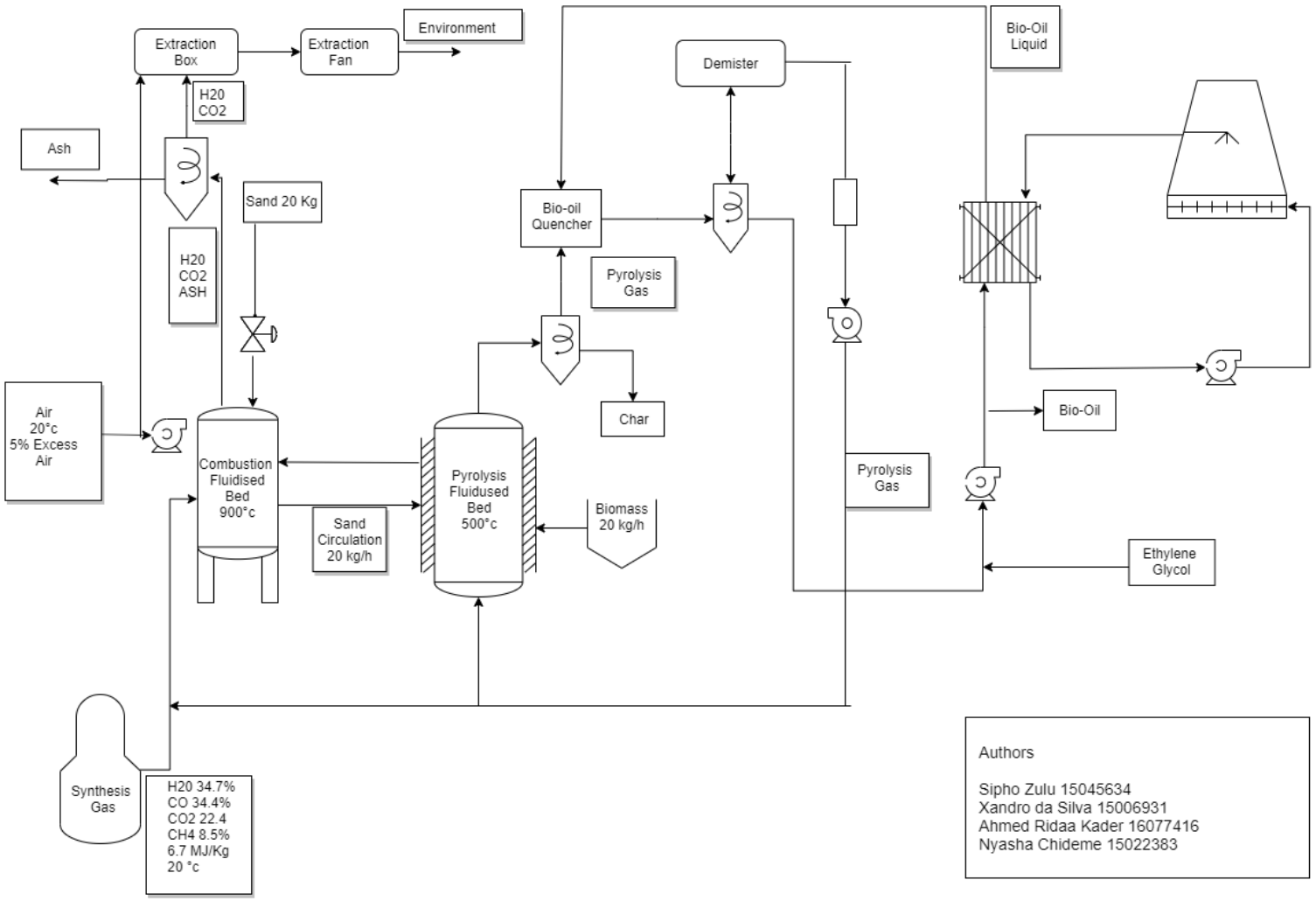

Figure A.1: Process Flow Diagram

B Reactor and heat exchanger

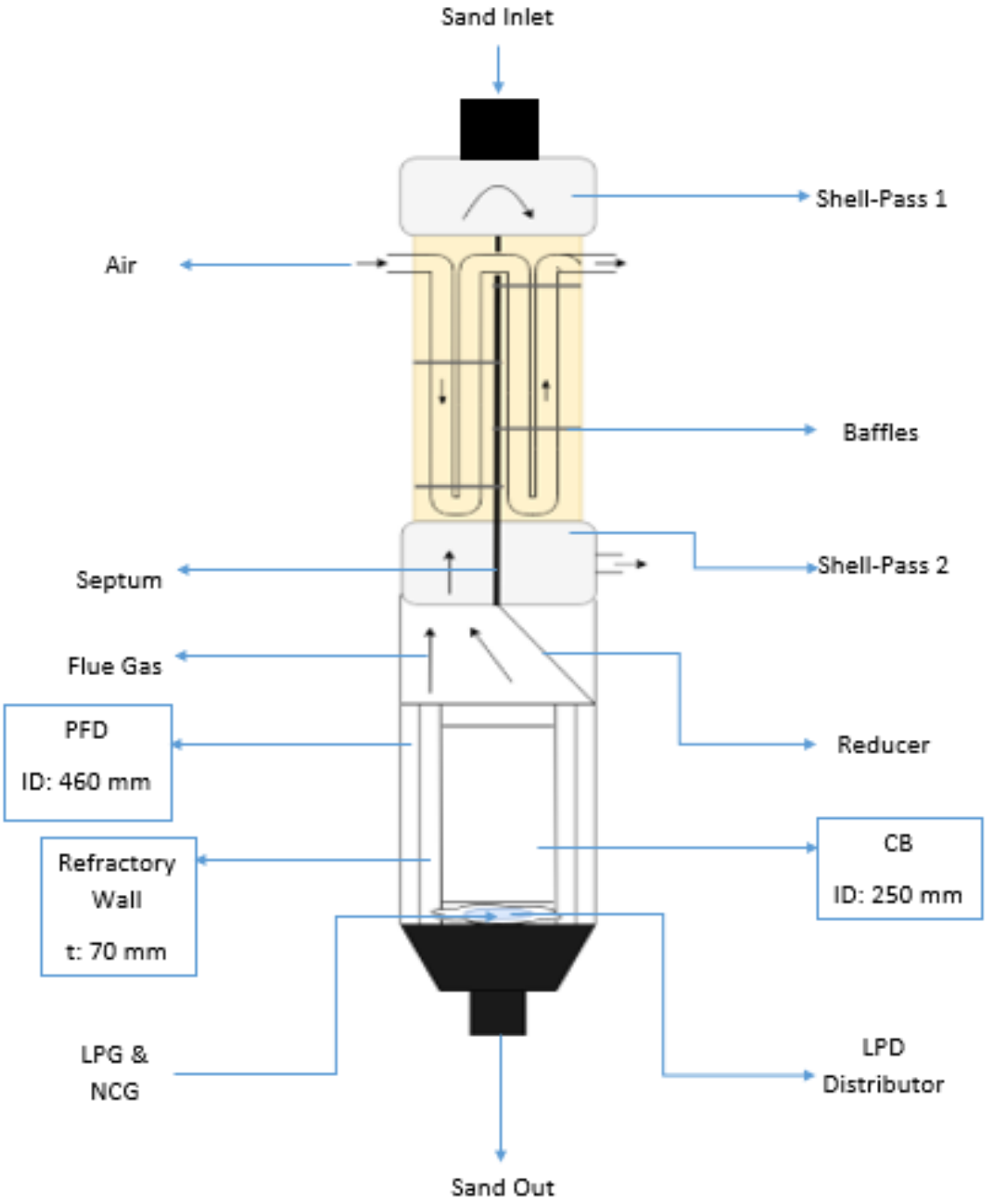

Figure B.2: Heat exchanger and reactor design. (Note: heat exchanger size is exaggerated for better clarity)